J|A|C|S COMMUNICATIONS

Published on Web 11/05/2009

Synthesis and Surface Modification of Highly Monodispersed, Spherical Gold Nanoparticles of 50−200 nm

Steven D. Perrault and Warren C. W. Chan*

Institute of Biomaterials and Biomedical Engineering, Terrence Donnelly Centre for Cellular and Biomolecular Research, University of Toronto, 160 College Street, Toronto, Ontario, Canada M5S 3E1

Received August 20, 2009; E-mail: warren.chan@utoronto.ca

Nanotechnology is now a central tool in biomedical research. Recent studies have focused on elucidating the impact of nanoparticle size and shape on biological systems, with implications for understanding nanotoxicity and the rational design of nanoparticles for medical use.[1−5] It is important that such studies use particles with homogeneous sizes and shapes, yet a model inorganic particle system in the 50−200 nm size range is currently unavailable. Here we demonstrate a method for synthesizing gold nanoparticles (GNPs) that provides a greater size range and better size and shape dispersion.

Typical GNP synthesis involves the chemical reduction of gold chloride using sodium borohydride and sodium citrate,[6] producing particles with sizes of 2−10 and 12−100 nm, respectively. Unfortunately, the citrate method can only produce quality particles up to ∼50 nm in size, beyond which they are polydispersed and nonspherical.[7] Reducing gold onto nanoparticle seeds (<15 nm) improves this,[7] but a substantial secondary population of smaller nanoparticles is formed in addition to growth of the seeds.[8] This could be overcome with an agent capable of selectively reducing Au only when in proximity to particle seeds. Hydroquinone (HQ) has a weak reduction potential ($E° = -0.699$ vs NHE),[9] and it is commonly used to selectively reduce silver (i.e., in film) because it is unable to spontaneously reduce Ag^+ ions that are isolated in solution (Ag^+/Ag^0, $E° = -1.8$ V) but can reduce Ag^+ in the presence of Ag^0 clusters or nanoparticles ($E° = +0.799$ V).[10,11] The reduction of gold is more complex because solubilized gold chloride includes a variety of species,[12] but Au^I appears to be highly stable. The difference between reducing gold chloride in the presence of metal clusters ($E° = 1.002$ V) and reducing isolated Au^I to Au^0 ($E°$ estimated to be -1.5 V)[13] could be substantial enough that the latter is nonspontaneous with hydroquinone. To test this, we examined the kinetics of HQ reduction of gold chloride in the presence and absence of particle seeds. At first we observed particle formation regardless of whether nanoparticle seeds were added. Gold chloride can be reduced by UV light, so a gold chloride solution may contain a fraction of Au^0 clusters. We centrifuged the stock solution at high speed for 60 min and examined the kinetics again, this time finding no particle formation until seeds were added (Figure 1a). This demonstrates the selectivity of HQ.

Next, we synthesized five nanoparticle batches using a consistent concentration of gold chloride but decreasing the number of seeds, which should result in the growth of larger particles. On the basis of the amount of gold chloride added, we determined the number of seeds required to produce particles with diameters of ∼50, 75, 100, 125, and 175 nm. As expected, addition of less seed resulted in longer absorption λ_{max} values, which is typical for increasingly larger GNP diameters (Figure 1b and Supplementary Figure 1 in the Supporting Information). Particle sizes determined from measurement of transmission electron microscopy (TEM) images were within several nanometers of the expected sizes, and a strong correlation between the quantity of nanoparticle seeds added and the final size was observed (Figure 1c).

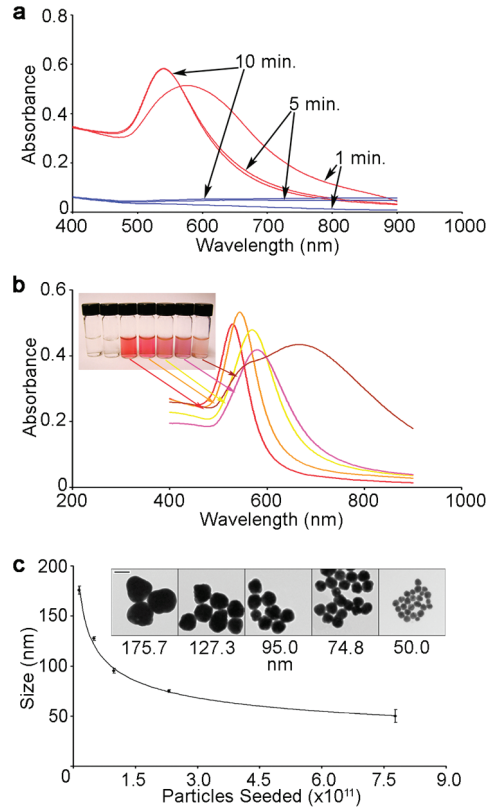

Figure 1. Reduction kinetics, seeding, and resulting particle sizes. (a) Complete ionic gold reduction (blue) is absent until particle seeds are added (red). (b) Absorption spectra of GNPs synthesized with various quantities of particle seeds. The inset shows (left to right) a sample with no HQ, another with HQ but no seed, and five samples with decreasing amounts of added seed. (c) The size of the GNPs was correlated with the number of input seeds. The inset shows representative TEM images of five sizes (scale bar = 100 nm).

We then synthesized large-diameter GNPs by the citrate method to allow a comparison against particles synthesized by HQ reduction (see the particle images in Supplementary Figure 2). The monodispersity of the citrate particles was poor (Figure 2a). With a mean diameter of 82.51 nm, their geometric standard deviation (σ_g) was 1.27. The monodispersity was improved with the HQ synthesis. Particles having a mean diameter of 84.95 nm had $\sigma_g = 1.09$. We also determined the longest-to-shortest axis lengths of GNPs formed by the two approaches as a measure of their shapes (Figure 2b). The citrate-synthesized population was less spherical, having a mean

10.1021/ja907069u

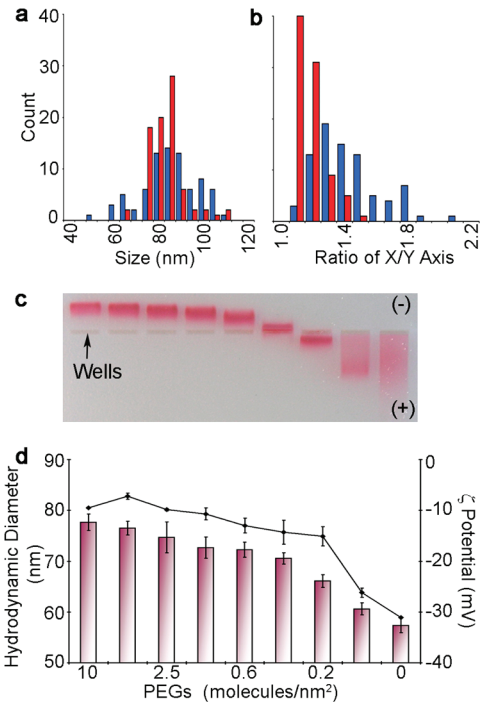

Figure 2. Comparison of citrate- and HQ-synthesized GNPs and pegylation of HQ-synthesized GNPs. (a) Histograms of the nanoparticle size dispersions and (b) ratios of long to short axis lengths show that citrate particles (blue bars) are more polydispersed and less spherical than the HQ particles (red bars). (c) Electrophoretic separation of 10× PEG to citrate particles (left to right) shows PEG-dependent migration. (d) Bar graph (left axis) shows increasing hydrodynamic diameter as more PEG molecules are added; line graph (right axis) shows a more positive ζ potential with more PEG.

ratio of 1.37 and coefficient of variation (COV) of 0.15, compared with a ratio of 1.13 and COV of 0.08 for the HQ-synthesized particles.

Two remaining considerations with respect to the HQ method are whether secondary nucleation occurs and the ease of modification for downstream studies. We found that inclusion of a low concentration (0.40−0.75 μM) of sodium citrate improved the monodispersity and stability, especially of large particles, but resulted in a small fraction (0.01−0.1%) of newly nucleated particles. Use of HQ alone grew particles with a low rate of new nucleation (<0.01%), but large-diameter particles were less monodispersed and aggregated within 24 h. Because the small amount of newly nucleated particles can be removed by centrifugation washes, we reasoned that a low concentration of citrate was advantageous for improving the overall batch quality.

Finally, we tested the ease of surface ligand exchange. The efficiency of particle pegylation (methoxy-PEG-thiol, MW = 5 kDa) was tested by incubating 50 nm GNP aliquots with various PEG-to-surface-area ratios. Separating the products by gel electrophoresis showed a shift from negative to positive charge as the PEG density increased (Figure 2c). The hydrodynamic diameter increased until saturation at 5−10 PEG/nm^2 (Figure 2d), and the ζ potential

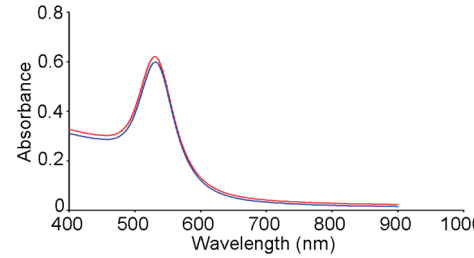

Figure 3. Filtering of raw (red) and pegylated (blue) 50 nm HQ-synthesized particles demonstrates that the samples are free of aggregates.

increased from −31.1 mV (citrate) to −7.2 mV (5 PEG/nm^2) (Figure 2d). These results are comparable to what we have observed using citrate particles. Following pegylation, the particles were easily concentrated by centrifugation. We also tested particle dispersion by passing them through a 0.22 μm filter before and after pegylation (Figure 3). The absorption λ_{max} decreased from 0.619 to 0.599, a 3.23% loss of nanoparticle concentration, suggesting that they are well-dispersed in solution.

In summary, GNPs synthesized using HQ have improved monodispersity and shape consistency in the 50−175 nm size range. Furthermore, we have synthesized nanoparticles with diameters of >200 nm. With this strategy and those of previous methods, we can now synthesize GNPs with a size range of 2−200 nms. This large range allows us to use GNPs as a model system to elucidate the nano−bio interface.

Acknowledgment. The National Sciences and Engineering Research Council of Canada supported this research through a research grant and a graduate scholarship for S.D.P.

Supporting Information Available: More representative images, data demonstrating that particles were not aggregated, and materials and methods. This material is available free of charge via the Internet at http://pubs.acs.org.

References

(1) Perrault, S. D.; Walkey, C.; Jennings, T.; Fischer, H. C.; Chan, W. C. W. *Nano Lett.* **2009**, *9*, 1909.
(2) Jiang, W.; Kim, B. Y. S.; Rutka, J. T.; Chan, W. C. W. *Nat. Nanotechnol.* **2008**, *3*, 145.
(3) Chithrani, B. D.; Ghazani, A. A.; Chan, W. C. W. *Nano Lett.* **2006**, *6*, 662.
(4) Fang, C.; Shi, B.; Pei, Y. Y.; Hong, M. H.; Wu, J.; Chen, H. Z. *Eur. J. Pharm. Sci.* **2006**, *27*, 27.
(5) Lundqvist, M.; Stigler, J.; Elia, G.; Lynch, I.; Cedervall, T.; Dawson, K. A. *Proc. Natl. Acad. Sci. U.S.A.* **2008**, *105*, 14265.
(6) Frens, G. *Nature, Phys. Sci.* **1973**, *241*, 20.
(7) Brown, K. R.; Walter, D. G.; Natan, M. J. *Chem. Mater.* **2000**, *12*, 306.
(8) Jana, N. R.; Gearheart, L.; Murphy, C. J. *Chem. Mater.* **2001**, *13*, 2313.
(9) Gentry, S. T.; Fredericks, S. J.; Krchnavek, R. *Langmuir* **2009**, *25*, 2613.
(10) Mostafavi, M.; Marignier, J. L.; Amblard, J.; Belloni, J. *Radiat. Phys. Chem.* **1989**, *34*, 605.
(11) Linnert, T.; Mulvaney, P.; Henglein, A.; Weller, H. *J. Am. Chem. Soc.* **1990**, *112*, 4657.
(12) Wang, S.; Qian, K.; Bi, X.; Huang, W. *J. Phys. Chem. C* **2009**, *113*, 6505.
(13) Gachard, E.; Remita, H.; Khatouri, J.; Keita, B.; Nadjo, L.; Belloni, J. *New J. Chem.* **1998**, *22*, 1257.

JA907069U